12

Improving the ion thruster scheme III. Optimization of the ion-optical system

© N.K. Fedyanin, A.A. Dyakov

Joint Stock Company „Keldysh State Research Center"(JSC Keldysh Research Center),
125438 Moscow, Russia
e-mail: nikita.fedyanin@gmail.com

Received October 9, 2024
Revised November 22, 2024
Accepted November 26, 2024

The current article describes the process of optimization of the ion-optical system based on the results of numerical modeling. The main objectives of the work are to increase the effective transparency of the ion-optical system for ions and expand the upper limit of the range of focused current densities. The optimization methods used are changing the shape of apertures from round to hexagonal, reducing the width of the bridges between the apertures and reducing the width of the grid-to-grid gap. The configuration of the ion-optical system created within the work has an advantage over the previously used one in all the main parameters except for the resource.

Keywords: electric propulsion, discharge chamber, ion optics, ion beam, ion cost, mass utilization efficiency.

DOI: 10.61011/TP.2025.01.60521.319-24

Introduction

Ion thrusters (IT) are among the most common types of electric rocket thrusters, which have characteristic high values of specific impulse and lifespan. The main components of the IT are a gas discharge chamber (GDC), responsible for the formation of plasma by shock ionization of the neutral component of the propellant by electrons, an ion-optical system (IOS) that extracts ions from the plasma of the GDC and creates thrust through their electrostatic acceleration, and a neutralizer that emits electrons into a beam of accelerated ions, compensating for its positive charge [1].

Most often, the IOS IT consists of an emission electrode (EE) and an accelerating electrode (AE), which are two plates made of refractory metal or carbon and perforated with circular apertures [2]. The ion beam is extracted, focused, and accelerated by applying a high potential difference to the electrodes. Electrons from the plasma of the GDC cannot overcome this potential difference, as a result of which charges are separated near the EE and a plasma boundary is formed, beyond which only ions penetrate into the space between the IOS electrodes. Plasma, called beam plasma, is also located outside the IT although in a lower concentration. To prevent the extraction of electrons from it, a potential barrier is created for them in the AE apertures by applying a potential lower than that of the plasma beam to the electrode [3]. The most common scheme of a single IOS cell and the potential distribution in it are shown in Fig. 1.

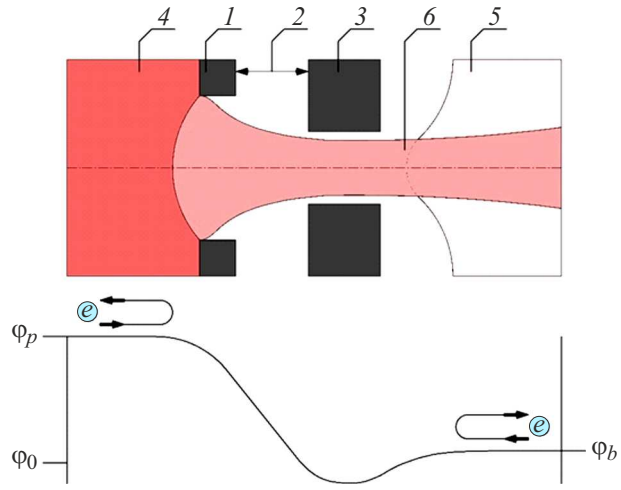

Figure 1. Scheme of a single IOS cell and potential distribution in it: *1* — EE; *2* — interelectrode gap; *3* — AE; *4* — GDC plasma; *5* — beam plasma; *6* — single ion beam; φ_p — GDC plasma potential; φ_b — beam plasma potential; φ_0 — the potential of the spacecraft body.

The effective transparency for ions of the IOS is one of its most important parameters. Ions that fall on the bridges between the EE apertures are neutralized on its surface and return to the GDC in the form of atoms, the re-ionization of which requires additional energy expenditure. The higher the effective transparency of the IOS, the lower the ion price, and the higher the efficiency of the thruster [4].

Another extremely important parameter of the IOS is its transparency for neutral atoms because the propellant in the GDC is not fully ionized. The lower this transparency, the higher the gas efficiency and the lower the flow rate of the propellant required by the thruster to achieve the required thrust. Some of the neutral atoms that have passed through the EE apertures return to the GDC after impact with the AE and for this reason their transparency is reduced mainly by lowering the geometric transparency of the AE by reducing the diameter of its apertures. Since the ions

Table 1. General parameters of the studied IOS configurations

Parameter	d_s, mm	d_a, mm	t_s, mm	t_a, mm	φ_p, V	φ_s, V	φ_a, V
Value	1.7	1.0	0.5	1.0	2030	2000	−300

Note. d_s — diameter of the circle inscribed in the EE aperture, d_a — diameter of the circle inscribed in the AE aperture, t_s — EE thickness, t_a — AE thickness, φ_p — GDC plasma potential, φ_s — EE potential, φ_a — AE potential.

in the IOS are not only accelerated, but also focused, a reduction of the geometric transparency of the AE, as a rule, does not prevent them from leaving the thruster [5].

Each IOS is capable of focusing a limited range of ion current densities, at which their trajectories do not intersect the surface of AE. Both the highest and lowest current densities of ions extracted from the GDC should fall within this range. Increasing the diameter of the AE apertures and reducing its thickness are the simplest ways to expand the range. The wider the range of current densities focused by IOS, the greater the thrust range can be achieved with constant IOS parameters [5].

This study is devoted to the continuation of the improvement of the IT scheme, the previous stages of which are presented in Ref. [1,6]. The results of a study of the main dependencies of the GDC parameters on the magnitude of the magnetic field induction and its topology were presented in the earlier papers of the cycle, and a technical solution was developed and tested that makes it possible to optimize these parameters independently of each other. The most obvious disadvantage of the ID-200PM, which was the subject of tests in previous studies, was the relatively low effective transparency of its IOS for ions. Thus, taking into account the existing groundwork, it is advisable to further improve the parameters of IT efficiency by improving its IOS. The aim of the this study is to optimize the IOS and, in particular, to increase its effective transparency for ions and expand the upper limit of the range of focused current densities. The optimization criterion is to maximize the above-mentioned parameters, corresponding to the current capabilities of the production base, which will ensure the mechanical strength of the IOS, as well as its resistance to high-voltage breakdowns. The planned result of optimization of IT parameters comprise an increase of efficiency and thrust density.

1. Optimization methodology

Several main parameters of the studied IOS configurations were compared in this study: effective transparency for ions, transparency for neutral atoms, and the range of focused current densities. Single cells of IOS configurations were modeled in the IOS-3D software package for calculating the parameters [7]. The fluxes of single-charged xenon ions were calculated, the initial velocities of which at the entrance to the simulation area were directed perpendicular to the EE plane. The modulus of the initial velocity was set equal to the minimum velocity of the Bohm criterion $v_{i0} = \sqrt{kT_e/M_i}$ at the thermal energy of electrons in the plasma $kT_e = 5\,\text{eV}$. The main algorithms of the program, including the plasma emitter modeling method, are described in Ref. [8]. The general parameters of the IOS, which are not changed in all developed configurations, are listed in Table 1. The potentials and thicknesses of the electrodes are borrowed from the basic configuration of IOS of ID-200PM [9], since the IOS is optimized at a fixed ion velocity in the beam in this study. The effect of the AE potential on the focusing of the ion beam is insignificant because of its small absolute value, in addition, the range in which this value can vary is extremely narrow, therefore, the optimization of the AE potential has not been carried out at this stage of work.

It is assumed that titanium will be used as an EE material in all studied IOS configurations. The transition from a carbon-carbon composite material to titanium is attributable to the higher strength properties of hard-melting metals and, as a result, a higher limiting geometric transparency. The change of the EE material does not have any negative effect on the parameters of the IOS and the thruster as a whole, however, it requires taking into account thermal deformations when designing it, since titanium has a temperature coefficient of linear expansion of about $9 \cdot 10^{-6}\,\text{K}^{-1}$, and the temperature coefficient of linear expansion of carbon is less than $2 \cdot 10^{-6}\,\text{K}^{-1}$. These deformations can be ignored when designing an IT with a small diameter of the perforated area of the IOS. If the diameter is over 100 mm, a convex shape is given to them so that their deflection arrows are directed in one direction to maintain the stability of the gap between the electrodes when the thruster is heated.

The AE material is less important in this study because the geometric transparency of this electrode is not increased. Titanium is also the intended material of all the studied configurations, but it can later be replaced with some carbon-based material, if necessary, to extend the IOS lifespan.

2. Electrode perforation

Effective transparency for ions depends on a variety of parameters, including the ratio between the ion current density and the potential difference between the electrodes, the thickness of the EE, the width of the interelectrode gap, the potential difference between the EE and the GDC plasma, etc. The effective transparency most obviously depends on the geometric transparency of the EE and the

Table 2. Parameters of IOS configurations with different perforations

Parameter	Shape of EE and AE apertures	l_a, mm	w_s, mm	Δj_{Xe}, A/m^2	τ_n, %
Configuration C	Circle	1.0	0.5	10–190	8.5
Configuration 5	Hexagon	1.0	0.5	10–170	9.5
Configuration 4	Hexagon	1.0	0.4	10–180	10.5
Configuration 3	Hexagon	1.0	0.3	10–170	11.6
Configuration 2	Hexagon	1.0	0.2	10–180	12.9
Configuration 1	Hexagon	1.0	0.1	10–170	14.8

Note. l_a — width of the interelectrode gap, w_s — width of the bridge between the EE apertures, Δj_{Xe} — range of focused current densities of xenon ions, τ_n — transparency for neutral atoms.

possibility and expediency of changing the shape of the apertures and reducing the width of the bridges between them were studied in this paper for increasing the EE geometric transparency.

Currently, EE perforation with circular apertures, the centers of which are located at the nodes of the hexagonal lattice, has become the most widespread. This aperture shape is traditional and has been used for over 60 years [10]. The choice of a round shape is primarily attributable to the fact that generally the electrodes were previously perforated by boring. The apertures of modern IOS have a much wider range of possible shapes because the laser cutting is the most common perforation method nowadays. Considering that the apertures are located in the nodes of the hexagonal lattice, the openings having a hexagonal shape will have an obvious advantage in terms of geometric transparency of the EE, since the area of the hexagon is about 10% higher than the area of the circle inscribed in it.

The main parameters of configurations with different perforations and the dependence of their effective transparency for xenon ions on the density of their current from the GDC to the EE, obtained from the results of numerical modeling, are presented in Table 2 and in Fig. 2, respectively.

Samples with perforations corresponding to EE configurations 3, 2 and 1 were made to evaluate the technological

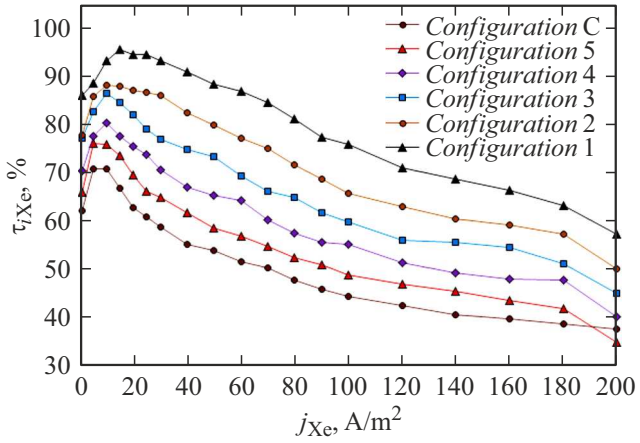

Figure 2. Dependences of the effective transparency of IOS configurations with different perforations for xenon ions τ_{iXe} on the density of their current from GDC to EE j_{Xe}.

feasibility of using the hexagonal shape of the apertures and reducing the width of the bridges between the EE apertures. The samples were made of titanium and had a thickness of 0.5 mm. The samples were perforated using a three-axis laser machine in an argon medium. Configuration 1 was not further considered because part of the bridges between the apertures was completely burnt out in sample with a bridge thickness of 0.1 mm during the cutting process. The appearance of perforated samples with bridge thicknesses of 0.2 mm (EE Configuration 2) and 0.3 mm (EE Configuration 3) is shown in Fig. 3.

The inspection found a burring characteristic of laser cutting on both perforated samples. Configuration 3 was chosen for further optimization at the current stage due to high probability of damaging the EE of Configuration 2 during deburring. Despite the fact that this configuration is only an intermediate link in the optimization process, its parameters already significantly exceed the parameters of the IOS used in Ref. [1,6]: transparency for neutral atoms has been reduced from 17 to 11.6%, and effective transparency for ions has been increased by more than 5%.

3. Width of the interelectrode gap

The second stage of the IOS optimization consisted in reducing the width of the interelectrode gap for increasing the electric field strength in the accelerating layer. As the voltage increases, the effective transparency of the IOS for ions increases, and the range of focused current densities expands to higher values, which makes it possible to increase the thrust density of the thruster. The maximum strength is limited by several factors, the most important of which is the resistance of the IOS to high-voltage breakdowns: the electric field strength in the interelectrode gap should not exceed a certain limit value at which regular breakdowns or a discharge occur between the EE and the AE.

Experimental studies show that IOS with electrodes made of molybdenum or carbon can properly function with an electric field strength in the interelectrode gap of at least 5 kV/mm hboxjcite5,11-13. At the same time, the electric field strength between EE and AE of the majority of modern IT, such as NSTAR [14], T6 [15], RIT-10 [16],

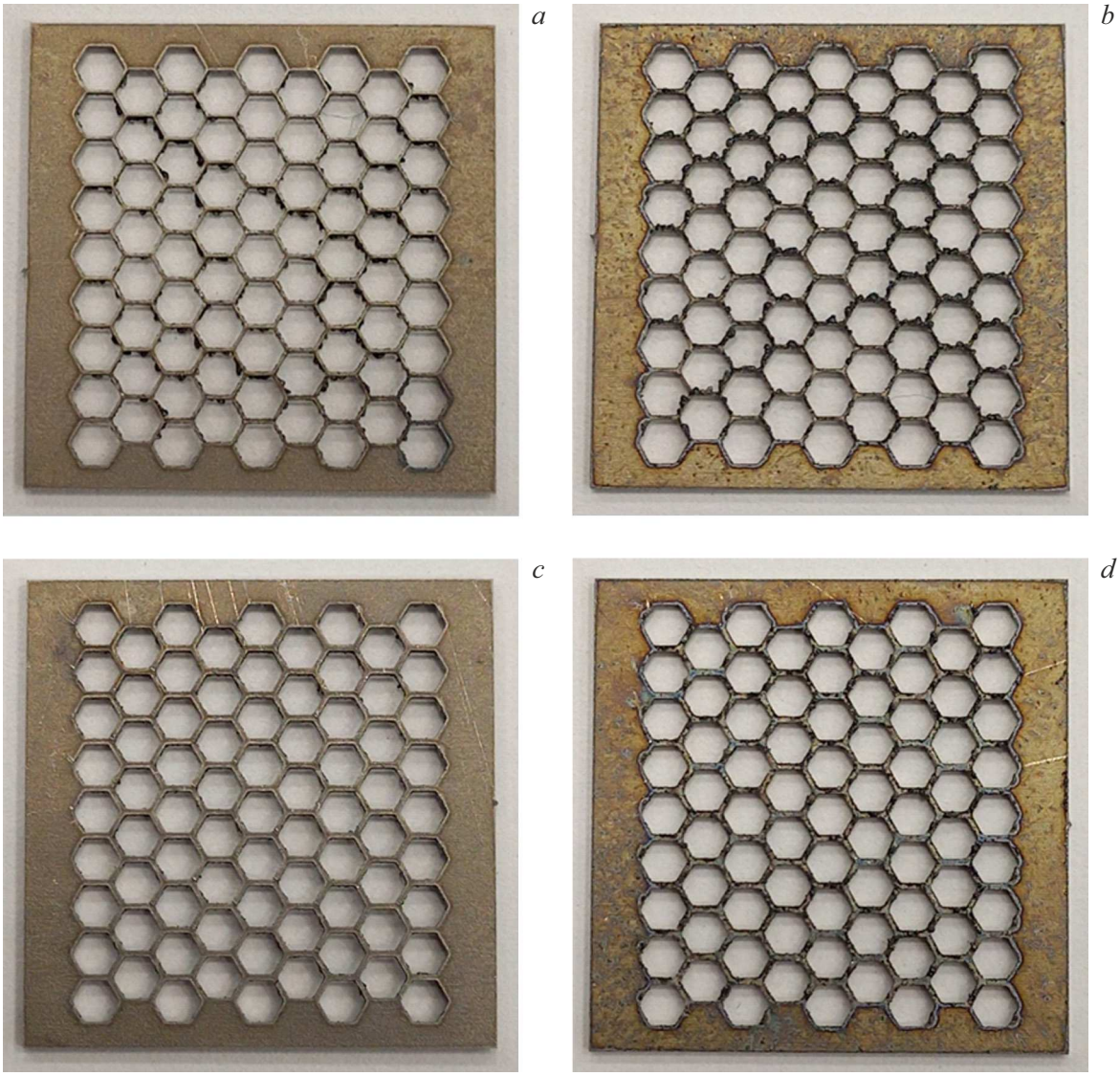

Figure 3. Appearance of perforated samples with different bridge thicknesses: *a* — 0.2 mm, front side; *b* — 0.2 mm, back side; *c* — 0.3 mm, front side; *d* — 0.3 mm, back side.

Table 3. Parameters of IOS configurations with different width of interelectrode gap

Parameter	Shape of EE and AE apertures	l_a, mm	w_s, mm	Δj_{Xe}, A/m^2	τ_n, %
Configuration 3	Hexagon	1.0	0.3	10–170	11.6
Configuration 5	Hexagon	0.5	0.3	10–280	12.0

Note. l_a — width of the interelectrode gap, w_s — width of the bridge between the EE apertures, Δj_{Xe} — range of focused densities of xenon ions, τ_n — transparency for neutral atoms.

IT-200KR [9] and etc., does not exceed 2.5–2.7 kV/mm. The choice of such values is most often attributable to the need to ensure resistance to high-voltage breakdowns with an uncontrolled decrease of the gap caused by thermal deformations of the electrodes and inaccuracy of assembly. If the assembly quality allows setting the required gap width with sufficient accuracy, and the thermal deformations are small or can be accurately calculated, the electric field strength between the electrodes can be set significantly higher than 2.5 kV/mm.

An experiment was conducted with a set of titanium plates to determine the maximum electric field strength between electrodes made of titanium. Both plates with and without perforation were used in the experiment. The plates were polished before the experiment to reduce the number of voltage concentrators on their surfaces. The plates in

the vacuum chamber were secured relative to each other at a certain distance, after which a potential difference was applied between them. The potential difference increased from 0 to the value at which the breakdown occurred, in 500 V increments. An excessive potential difference was applied to the plates before the experiment to initiate multiple breakdowns for removal of roughness, oxide films and impurities. The maximum potential difference at which no breakdowns between the plates were recorded was 6 and 10 kV in the pressure range from $5 \cdot 10^{-4}$ to $5 \cdot 10^{-2}$ Pa with 0.5 and 1 mm gaps between the plates, respectively. The obtained result is almost identical for both perforated and non-perforated plates and is similar to the results of a similar experiment with a set of molybdenum plates described in Ref. [5]. A margin coefficient with the value in the range from 1.5 to 2 should be used in accordance with the quantitative estimates presented in Ref. [5] in case of transition from plates to IOS electrodes. If the margin coefficient is 2, the limiting electric field strength for titanium will be 6 kV/mm with an interelectrode gap of 0.5 mm and 5 kV/mm with a gap of 1 mm.

Since the potential difference between EE and AE in this work is 2.3 kV, taking into account the results of the measurements, the width of the interelectrode gap in the developed IOS configuration can be reduced up to a value of 0.4 mm. Nevertheless, the gap was reduced only to 0.5 mm in further calculations to compensate for inaccuracies that may occur in case of subsequent assembly of the IOS.

The effectiveness of the reduction of the gap width was evaluated by comparing Configurations 3 and 5. The main parameters of the configurations and the dependences of their effective transparency for xenon ions on the density of their current from the GDC to the EE, obtained from the results of numerical modeling, are provided in Table. 3 and on Fig. 4, respectively.

The advantage of Configuration 5 is obvious according to the results of comparison. This configuration allows

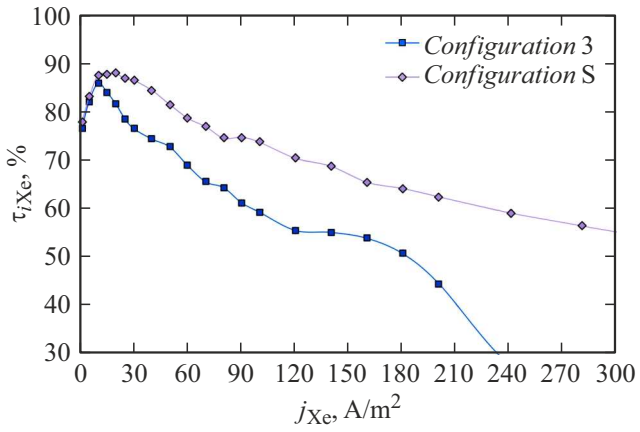

Figure 4. Dependences of the effective transparency of IOS configurations with different width of the interelectrode gap for xenon ions $\tau_{i\mathrm{Xe}}$ on the density of their current from GDC to EE j_{Xe}.

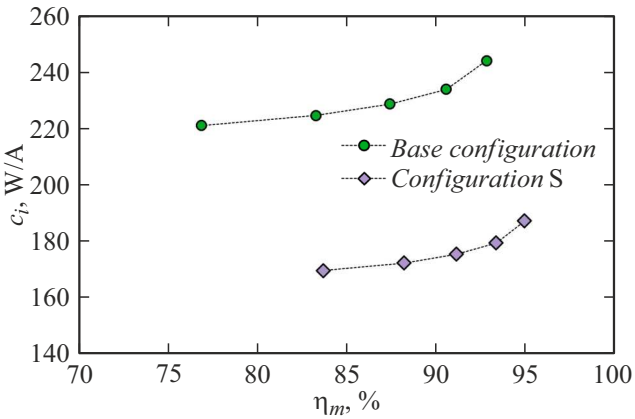

Figure 5. Dependences of ion price c_i on gas efficiency η_m (efficiency curves) for various configurations of IOS.

for increasing the effective transparency for ions by more than 10% and raise the upper limit of the range of focused current densities by 65%, without any significant negative impact on other parameters of the IOS. The main disadvantage of Configuration 5 is the average increase by 5° of the half-angle of the ion beam divergence, which, however, does not significantly affect the IT parameters as a whole.

The advantages of Configuration 5 are more clearly demonstrated in Fig. 5. The first dependence of the ion price on gas efficiency was obtained experimentally and corresponds to the lowest values of the ion price achieved by ID-200PM in the studies covered in Ref. [1,6]. The transparency of the initial configuration of ID-200PM IOS for neutral atoms and its effective transparency for xenon ions during firing tests were about 17 and 63%, respectively. The second curve was obtained by calculation and corresponds to thruster ID-200PM, in which its original IOS configuration was replaced by Configuration 5. The linear dependence of the ion price on the effective transparency for ions described in Ref. [4] was used for calculating this curve.

The evaluation shows that Configuration 5 can reduce the price of the ion price of ID-200PM by 25% with a gas efficiency of 90%. In this case, ID-200PM will have the lowest ion price among all existing similar thrusters with a diameter of the perforated area of the IOS up to 300 mm, with the exception of the XIPS-25 IT, information about which is insufficient to analyze the parameters it has achieved.

The combination of increased effective transparency for ions and a high upper range of focused current densities of the developed IOS configuration is likely to also allow the IT to achieve significantly higher thrust densities. The maximum beam current density that the initial configuration of ID-200PM IOS can extract from the GDC is 73 A/m^2 with 0.1 mm misalignment of the EE and AE apertures.. Configuration 5 with a similar misalignment can extract 115 A/m^2, which is 57% greater. In the

case of successful implementation of the developed IOS configuration, in some operating modes, the IT will be able to achieve thrust almost identical to a Hall thruster of a comparable size.

The estimation of the lifespan of the developed IOS configuration is the most urgent task at the moment. Configuration 5 and the basic configuration of ID-200PM IOS will have an almost identical lifespan with equal ion beam current densities and identical AE materials. Since the diameter of the AE aperture in Configuration 5 is smaller, optimizing the AE potential at subsequent stages of operation will increase the lifespan.

The problem of ensuring the lifespan of the IOS remains unresolved at increased ion beam current densities that can be extracted from the GDC with Configuration 5. It will be necessary to introduce new technical solutions into the configuration or use a AE made from a carbon-based material for providing a lifespan of more than 10 000 h with a xenon ion beam current density of more than 50 A/m^2.

Conclusion

This paper describes the process of optimizing the IOS based on the results of numerical modeling. The main objectives of the study are to increase the effective transparency of the IOS for ions and expand the upper limit of the range of focused current densities. The optimization process is divided into two stages. The geometric transparency increases at the first stage as a result of changing the shape of the apertures from round to hexagonal and reducing the width of the bridges between the apertures. The width of the interelectrode gap is reduced at the second stage.

All main parameters of the IOS configuration designed in the study surpass the parameters of previously used configuration, with the exception of the lifespan. The estimation shows that replacement of the initial configuration of ID-200PM IOS with Configuration 5 can reduce the ion price of the thruster by 25% with a gas efficiency of 90%. The combination of increased effective transparency for ions and a high upper range of focused current densities of the developed IOS configuration is likely to also allow the IT to achieve significantly higher thrust densities. However, the problem of ensuring the lifespan of the IOS extracting increased ion beam current densities from the GDC remained unresolved.

Acknowledgments

The authors would like to thank A.A. Shagaida for his help in carrying out the calculations.

Conflict of interest

The authors declare that they have no conflict of interest.

References

[1] N.K. Fedyanin, M.Yu. Selivanov, D.A. Kravchenko, A.V. Sabitova. ZhTF, **94** (11), 1897 (2024) (in Russian). DOI: 10.61011/JTF.2024.11.59107.80-24
[2] M. Sangregorio, K. Xie, N. Wang, N. Guo, Z. Zhang. Chinese J. Aeronautics, **31** (8), 1635 (2018). DOI: 10.1016/j.cja.2018.06.005
[3] E.V. Pawlik, P.M. Margosian, J.F. Staggs. NASA Tech. Note, NASA TN D-2804, 1965.
[4] D.M. Goebel, J.E. Polk, A. Sengupta. 40th AIAA/ASME/SAE/ASEE Joint Propulsion Conf. and Exhibit, 2004-3813, 2004. DOI: 10.2514/6.2004-3813
[5] D.M. Goebel, I. Katz. *Fundamentals of Electric Propulsion* (John Wiley & Sons, Inc., 2008), DOI: 10.1002/9780470436448
[6] N.K. Fedyanin, D.A. Kravchenko, M.Yu. Selivanov, A.V. Sabitova. ZhTF, **94** (12), 2159 (2024) (in Russian).
[7] A.A. Shagayda. *Simulation of charged particles in the ion-optical systems of ion engines* (IOS-3D), Software Package, Ver. 2.0. Certificate of official registration № 2014610277, 2014.
[8] A.A. Shagayda, V.V. Nikitin, D.A. Tomilin. Vacuum, **123**, 140 (2016). DOI: 10.1016/j.vacuum.2015.10.030
[9] S.V. Madeev. *Eksperimental'noe issledovanie elektrodov ionno-opticheskikh sistem ionnykh dvigatelej iz perspektivnykh uglerodnykh materialov* (Dissertaciya, 2020) (in Russian)
[10] W.R. Kerslake, E.V. Pawlik. NASA Technical Note, NASA TN D-1411, 1963.
[11] M. Nakano, Y. Kajimura, I. Funaki. Transactions Jpn. Society Aeronautical Space Sci., **10** (ists28), Pb_85 (2012). DOI: 10.2322/tastj.10.pb_85
[12] I. Funaki, H. Watanabe, M. Nakano, Y. Kajimura, T. Miyasaka, Y. Nakayama, H. Kuninaka, I. Shinohara. 48th AIAA/ASME/SAE/ASEE Joint Propulsion Conf. and Exhibit, 2012 (2012). DOI: 10.2514/6.2012-3797
[13] M. Nakano, K. Nakamura, Y. Naito, Y. Nakagawa, Y. Takao, H. Koizumi. AIP Advances, **9** (3), 035343 (2019). DOI: 10.1063/1.5090413
[14] J. Wang, J.E. Polk, J.R. Brophy, I. Katz. J. Propulsion and Power, **19** (6), 1192 (2003). DOI: 10.2514/2.6939
[15] N. Fazio, S.B. Gabriel, I.O. Golosnoy. Space Propulsion Conf., SP2018_00102, 2018.
[16] M. Tartz, H. Neumann. 42nd AIAA/ASME/SAE/ASEE Joint Propulsion Conf. and Exhibit, 2006-5001, 2006. DOI: 10.2514/6.2006-5001

Translated by A.Akhtayamov